Sound absorption of porous cement composites: Effects of the porosity and the pore size

Marius Rutkevičius,*[a] Zak Austin,[a] Benjamin Chalk,[a] Georg H. Mehl,[a] Qin Qin,[b] Philip A. Rubini,[b] Simeon D. Stoyanov[c] and Vesselin N. Paunov*[a]

[a] *Department of Chemistry, The University of Hull, Hull, HU6 7RX, UK*

[b] *The Acoustics Research Centre, School of Engineering, The University of Hull, Hull, HU6 7RX, UK*

[c] *Unilever R&D Vlaardingen, Olivier van Noortlaan 120, 3133 AT, Vlaardingen, The Netherlands*

E-mail: M.Rutkevicius@outlook.com; V.N.Paunov@hull.ac.uk; Fax: +44 (0)1482 466410; Tel: +44 (0)1482 465220

Zak.Austin@RB.com

benchalk@changeforce.com

g.h.mehl@hull.ac.uk

q.qin@hull.ac.uk

p.a.rubini@hull.ac.uk

simeon.stoyanov@unilever.com

Abstract

We used a hydrogel slurry templating technique to fabricate cement-hydrogel composites with a varying percentage of entrapped hydrogel microbeads of different size distribution. The air-drying of such composites allowed us to produce porous cement with controlled porosity and pore size matching the hydrogel bead distribution. We used hydrogel slurries prepared from Xanthan-Konjac gum mixtures with hydrogel bead size varying from 0.7-2.5 mm produced by mincing or blending. Porous cement composites were produced with porosity up to 80 vol% using these hydrogel slurries. The composites porosity, mass density, compressional strength and sound absorption properties were analysed. SEM analysis showed residual domains from the dried hydrogels beads within the voids created by the hydrogel bead evaporation in the cement samples. Sound absorption coefficient of the composite varied with the templated hydrogel bead size and the overall porosity. We found that the composite samples made with hydrogel beads of average size 0.7 mm showed high absorption coefficients between 0.5 and 0.80 for 500-800 Hz for 50 vol% porosity. Samples produced by templating hydrogels of 1 mm bead size and 70 vol% porosity showed an increased absorption over the sound frequency range 200 - 2000 Hz. Templating a mixture of the 1.6 mm and 1.0 mm hydrogel beads slurries with cement slurry did not appear to yield synergistic effect in the sound absorption of the produced porous composites compared to samples made from the separate slurries. The mechanical strength of the obtained porous cement composites seem to decrease with the increase of porosity.

Introduction

One of the problems which is increasing in severity as society makes advances is noise pollution [1]. Noise pollution is a serious health hazard, with a potential to cause hypertension, ischemic heart disease, severe hearing difficulties and even hearing loss if subjects are exposed to intensive noise for prolonged time [2, 3]. There are several methods for noise reduction: (i) passive, that relies on obstructing the noise using a barrier, and (ii) active, by interfering with the source of the sound waves [4, 5]. The former is the more common solution for noise reduction. A passive sound absorber requires no additional external power to operate in order to absorb sound. Sagartzazu et al. provide a review of many fundamental sound absorbing materials and the properties that make them effective [6]. Since sound energy is lost by air molecule friction, porous materials are ideal for the purposes of sound absorption [7]. The typical pore size of sound absorbing material is below 1 mm, which is much smaller than the wavelength of sound (5 cm –

15 m) [8]. The sound pressure creates oscillations between the gas molecules within the porous material, resulting in a frictional loss of momentum of these molecules. This way the porous structure reduces the momentum of the propagating high frequency sound wave [8]. Efficient conduction of heat within a porous composite results in an energy loss for a low frequency sound wave, as the air pressure in the pores oscillates resulting in a change of temperature [8]. In general, porosity, tortuosity and air flow resistivity have been claimed as the most important properties for the efficient sound absorption [9, 10]. Typical sound absorbing materials come in forms of polymer foams, fibres, boards, mats, perforated metals, aerogels and others [8, 11, 12].

It has been recently suggested that introducing another level of porosity, e.g. dual porosity may enhance the acoustic absorption of porous materials [13]. Introduction of slits within aerated autoclaved concrete samples showed to improve acoustic absorption by a factor 1.5-2 [14], as well as added holes in mineral wool [15]. More recently, instead of hole-drilling researchers started to incorporate various particles, such as hemp [16], reed [17] and polymer foam particles [18], within composite building materials in order to introduce different levels of porosity and improve the acoustic impedance of the material. Sound absorption generally increases with the increase in the sample thickness [17, 19] but the average pore size and the overall porosity also play a key role in the acoustic absorption. [5, 17, 19].

In our previous studies we have designed a versatile method for the fabrication of porous materials by hydrogel templating and analysed their acoustic absorption properties [20, 21]. A typical production mechanism is summarised in Fig. 1. A hydrogel is first prepared and set following by its blending into millimetre or sub-millimetre size gel beads and combining the resulting slurry with a cement slurry in one hydrogel – cement composite. The latter is then left to cure for at least 48 hours and the hydrogel is evaporated by air-drying, leading to voids within the composite. The method benefits of good control of the pore size and porosity, both which are controlled by the size and volume fraction of hydrogel beads used in the preparation of the composites. It is worth mentioning that the method is environmentally friendly, as the hydrogel is produced using natural plant extract and the drying can be conducted at ambient conditions without further energy expenditure. In the current paper we analyse the influence of the pore size on the acoustic absorption of the obtained porous cement composites. We also explored the sound absorption of cement composites of multiple porosity.

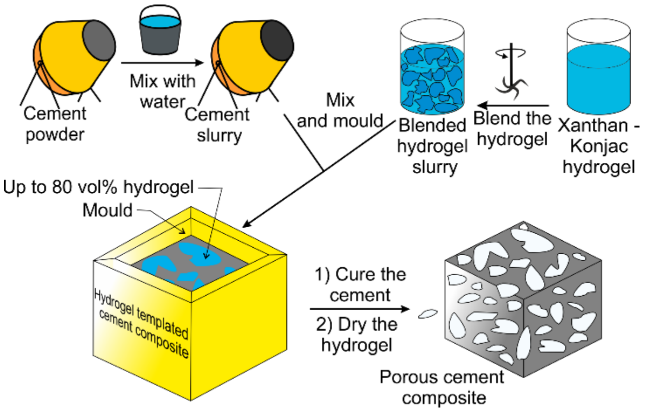

Fig. 1 Schematics showing the methodology of fabrication of porous cement using hydrogel bead slurry. A hydrogel is first prepared by hydration of the gelling agent in water followed by setting of the gel and its further blending or mincing it into a slurry of hydrogel beads. Separately, the cement powder is mixed with water to make a cement slurry. Then the hydrogel slurry is mixed with the cement slurry and the mixture is moulded. After the curing of the cement, the sample is dried in air to produce a porous cement composite. Note that the size of the hydrogel beads determine the pores size in the final porous composite.

Experimental procedure

Materials

Xanthan gum (Vanzan® NF) was kindly supplied by R. T. Vanderbilt Company, Inc., Norwalk, CT, USA, Konjac gum (Nutricol® GP 312) was supplied by FBC BioPolymer, Philadelphia, PA, USA. Lafarge extra rapid curing cement was purchased in a local store. Fluorescein disodium salt, microscopy grade and sodium azide, 99% were purchased from Sigma Aldrich, UK. Purified water with a conductance below 50 µS was used in all experiments.

Production of the hydrogel beads

To produce the hydrogel, 500 mL of water was first heated to 80 °C in a water bath. Xanthan gum (8.325 g) and Konjac gum (4.1625 g) were added and the solution was homogenised using an Ultraturrax homogeniser until a uniform solution was produced after 3-5 minutes of agitation. The hydrogel was then centrifuged for 3 minutes at 5000 × *g*, then reheated to 80 °C and centrifuged again, to remove trapped air bubbles. The mixture was then allowed to cool before being put into either a mincer (a mincer attachment used with Kenwood Chef mixer) with 2 mm or 3 mm sized mincer plate holes or a blender (a Kenwood Soup blender equipped with three stacked blades within the device) to produce hydrogel beads. We used the original 3 mm holes size mincer plate supplied by Kenwood and also a 2 mm hole size plate which was made in house. In order to make hydrogel beads, the hydrogel slurries were put through the mincer more than once, they were labelled with the number of passes (1-4), 'minced once, twice…', etc. For hydrogels slurries prepared in a blender, the hydrogel was blended for a total of two minutes at full power to produce a smaller hydrogel bead size. This type of hydrogel slurries were labelled as 'Blended'.

In additional experiment, sodium alginate hydrogel beads were produced by a drop-wise addition using a plastic syringe with a standard needle (rate 0.5 cm^3 min^{-1}) of the pre-hydrated hot 4 wt% sodium alginate solution into a beaker containing 10 wt% of calcium chloride. The alginate hydrogel beads were then drained and used in composite production without further mixing or blending.

Production of cement composites

The cement powder was mixed with water in a 2.175:1 ratio to form a cement slurry and then mixed with varying amounts of hydrogel bead slurries to produce the different cement-hydrogel composites. These slurries were put into a Teflon cast of 76 mm inner diameter (the same as the diameter of the impedance tube) and a thickness of 20 mm, ensuring the surfaces as flat as possible. The solidified casts were covered with a piece of damp paper towel and then foil to slow the drying process. After two days the casts were moved to an oven at around 70 °C to dry for at least five days to constant weight.

Particle size analysis

Microscope images were captured with Olympus BX-51 optical microscope in brightfield light fitted with DP70 CCD camera and the particle sizes were analysed using an image analysis software Image Pro Plus 6. Blended hydrogel beads were analysed using Malvern Mastersizer 2000. Scanning electron microscope (SEM) images were obtained using a bench-top Hitachi TM-1000 SEM. Samples for analysis were prepared by attaching them onto an adhesive carbon sticker, which was pre-attached onto an aluminium SEM stub (Agar, UK). None of the samples were coated prior to their examination.

Mechanical Strength Test

The samples were subject to mechanical strength testing using a Lloyds LD100 testing apparatus equipped with a 100 kN cell. The compression speed was set to 4 mm s^{-1}. Force at break point was used to calculate the compressional strength.

Sound absorption analysis

To determine the porous composite sample acoustic properties, i.e. the sound absorption ability, samples were analysed with an acoustic impedance equipment. The measurement revealed the materials performance in terms of sound absorption. Composite samples were inserted into an acoustic impedance tube and their sound absorption coefficients were analysed at different sound frequencies. An impedance tube with a single microphone was used in this test, where the microphone was attached to a slider according to the published standards [22]. The sound impedance tube was made from aluminium, its inner diameter was 76 mm and the distance from the sound source to the plunger was 3.0 meters. Computer based software analysed the measured sound pressure amplitude of the combined waves (the sum of the incident wave and the reflected wave). The slider was used to change the position of the microphone within the tube to find the highest (MAX) and the lowest (MIN) sound pressure of the combined waves. The collected p_{MAX} and p_{MIN} pressures were then used to calculate the sound absorption coefficient, α, using the equation

$$\alpha = 1 - \left\{ \frac{[(p_{MAX} / p_{MIN}) - 1]^2}{[(p_{MAX} / p_{MIN}) + 1]^2} \right\}.$$

The lower frequency for the test was set to 200 Hz and the upper to 2000 Hz. Data points were taken every 50 Hz for frequencies below 500 Hz, then up to 1000 Hz every 100 Hz and every 200 Hz for the higher frequencies.

Results and discussion

Hydrogel bead size analysis

In order to control the properties of the samples, it was important to investigate a method of controlling the average hydrogel beads size, which determined the average size of the pores in the porous composites. Upon production of hydrogel beads using the mincing method, a distribution range of the bead sizes to vary the bead size was obtained by analysing fluorescent microscope images of the hydrogel beads stained with a small amount of fluorescein disodium salt. The proposed method for hydrogel bead size control was to use mincer plates with differently sized holes for the mincer attachment (2 mm and 3 mm). After passing the hydrogel through the 2 mm size hole attachment once produced 1.6 ± 0.6 mm beads and the 3 mm attachment produced 2.5 ± 0.8 mm beads (see Fig. 2). The data in Fig. 2 shows that use of different mincing techniques allowed control over the hydrogel bead size.

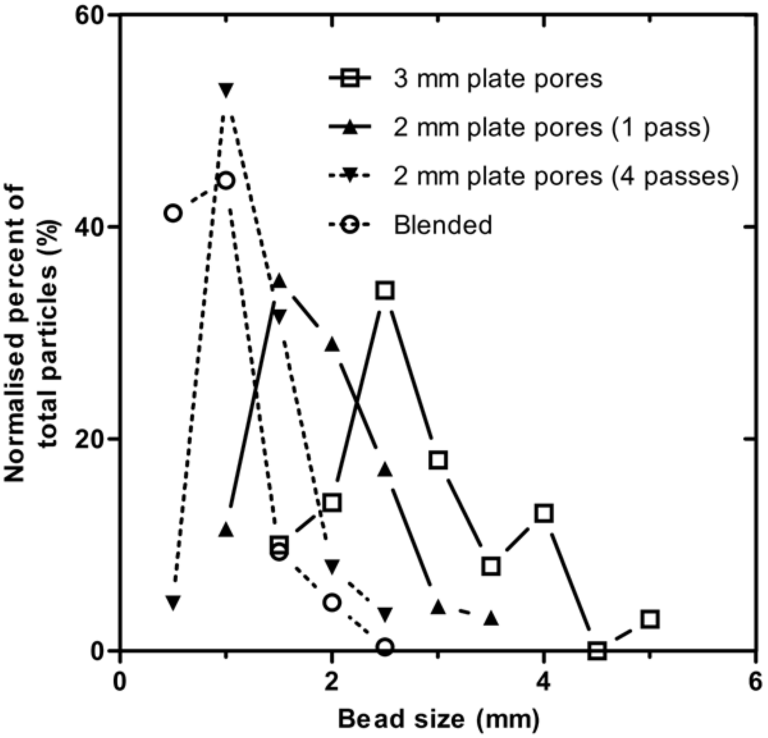

Fig. 2. Particle size distribution of the minced hydrogel beads, after passing it through a mincer plate of pore size 3 mm (□) and 2 mm (one pass - ▲, four passes - ▼) adjacent to the mincer blade; the sample, where the hydrogel was blended with a blender (○).

To further reduce the size of the hydrogel beads, we passed the hydrogel multiple times through the 2 mm hole size mincer plate. As it can be seen from the Fig. 2, as the hydrogel passed the mincer multiple times, the average size of the beads decreased. The average bead size for the "once minced" hydrogel was 1.6 ± 0.6 mm, which deceased to 1.0 ± 0.4 mm for the four times minced hydrogel. Due to the large size difference these two sizes were selected to be compared in the composite cement-hydrogel samples both individually and in a mixture in 1 : 1 ratio. The average bead size of the 'blended' hydrogel slurry 0.7 ± 0.7 mm. Here the standard deviations characterize the polydispersity of the samples. The different beads size determined the size of the pores in the porous cement, as the cement matrix solidified around the trapped hydrogel beads. Once the samples were cured the water from the beads was evaporated, leaving a cavity in the place of the hydrogel bead.

The hydrogel bead size is determined the porous structure of dried composite sample as shown in Fig. 3. As the hydrogel bead size was reduced, smaller pores were observed. As expected, the increase in the amount of hydrogel used increased the porosity (see e.g. Fig 3d).

Very small volume shrinkage of the composite porous samples was observed for initial hydrogel volume fractions below 70% after drying. However, we observed shrinking of samples where obtained with the smallest sized hydrogel beads at 80 vol%, where 2 mm pore size plate was used (bead size 1.0-1.6 mm), as well as for samples prepared with 70 vol% and 80 vol% blended hydrogel beads (bead size 0.7 mm). These composites reduced their volume during the drying stage, as there was not enough interconnectivity between the cement matrix. Due to the capillary pressure of the aqueous phase in the drying structure, it ruptured and shrank during the of water evaporation, similar to the process of drying of aerogels without prior solvent exchange steps [23]. To strengthen the cement matrix, we also allowed the cement-hydrogel samples of very high hydrogel beads content to cure for two weeks without evaporating the hydrogel. However, the extended curing time did sustain the composite volume without further shrinking upon the complete evaporation of water from the hydrogel beads.

The composite samples made with larger hydrogel beads (where 3 mm pore size mincer plate was used) did not shrink even at 80 vol% of the hydrogel as the cement matrix hardened in the voids between the hydrogel particles and form strong a scaffold structure strong enough bonds to support the composite in the drying step.

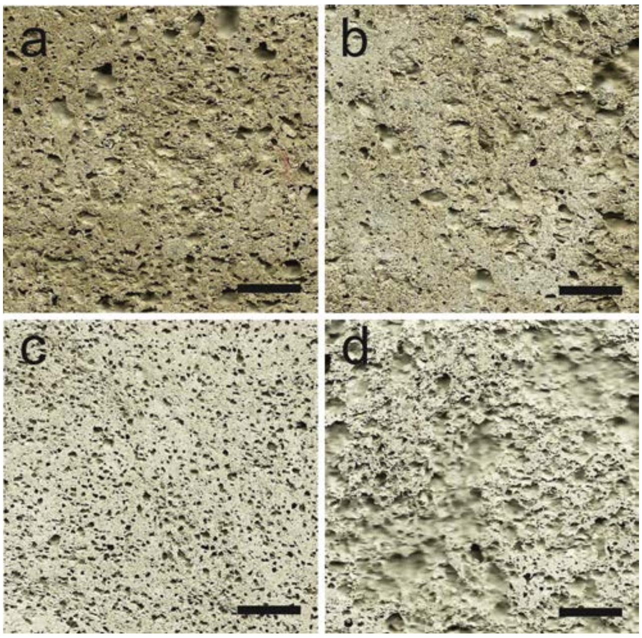

Fig. 3 Photographs of porous cement composites where (a-c) 50 vol% hydrogel was used: (a) minced once hydrogel, (b) a combination of minced once and four times (1:1 w/w ratio) hydrogel slurry, (c) blended hydrogel, and (d) 70 vol% hydrogel of the combined minced once and four times (1:1 w/w ratio). Scale bar is 500 µm.

Porosity of the composites

The porosity of the composites, θ, was calculated using the following formula

$$\theta = \left(1 - \frac{\rho_0}{\rho_s}\right) \times 100\%$$

where ρ_0 is the apparent density of the porous composite, calculated from the volume and mass after drying the samples and ρ_s is the density of the pure matrix without the hydrogel.

It can be seen from Fig. 4(a) that the density of the porous samples decreased with the increased hydrogel beads content. A slightly lower mass density of the cement-hydrogel composite was measured when blended hydrogel slurry was used instead of a minced one. The porous composite density did not decrease linearly from 0 vol% to 50 vol% initial hydrogel content. This can be seen more clearly from the calculated sample porosity as presented in Fig. 4(b). The increase in porosity did not directly match the hydrogel content within the composites and the offset was about 5-15 % away from a linear regime. This can be attributed to a hydrogel syneresis and release of water from the hydrogel beads into the cement slurry at the moulding stage due to osmotic pressure misbalance of the aqueous media in the cement slurry and that of the hydrogel. Another possibility is that some of the water remained bond within the samples and cannot be removed during the drying step. For larger hydrogel bead size, i.e. 2.5 mm, the weight loss data was more consistent with the increase in porosity through the evaporation of hydrogel.

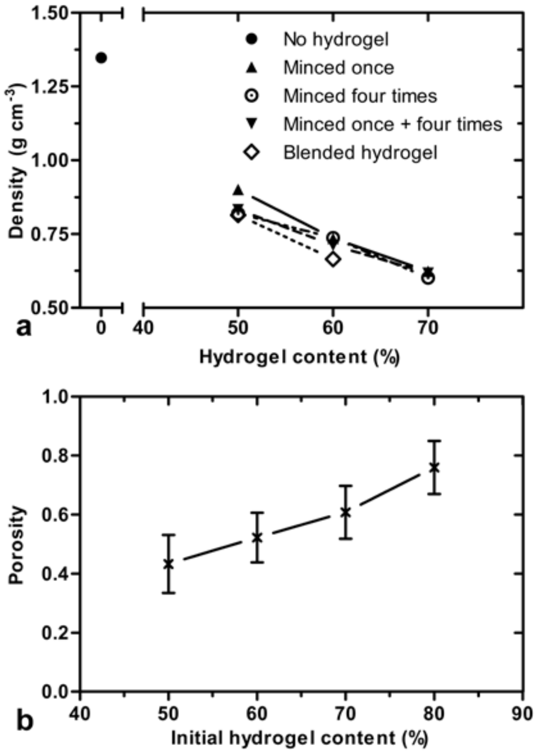

Fig. 4 a: Porous composite mass density vs. the initial hydrogel content within the samples. Mincer plate with 2 mm holes was used. b: Porosity as a function of the initial hydrogel content within the composites. The data of all types of hydrogel beads were averaged and the errors represent standard deviation. The data point at 80 vol% represents only the sample where 3 mm pore size mincer plate was used.

SEM analysis

SEM images of the cement composites with evaporated Xanthan – Konjac hydrogel slurries are displayed in Fig. 5 (a-c). Pores within cement can be observed in all of the samples. The micrographs show the microstructures formed around pores in the cement which were filled with the hydrogel residue. The images show pores partly coated by the residual gelling agent, where the hydrogel beads were trapped. This may have an implication on the way this material absorbs sound by additional viscous dampening of the sound energy which could potentially yield an increased absorbance at their specific resonance frequencies.

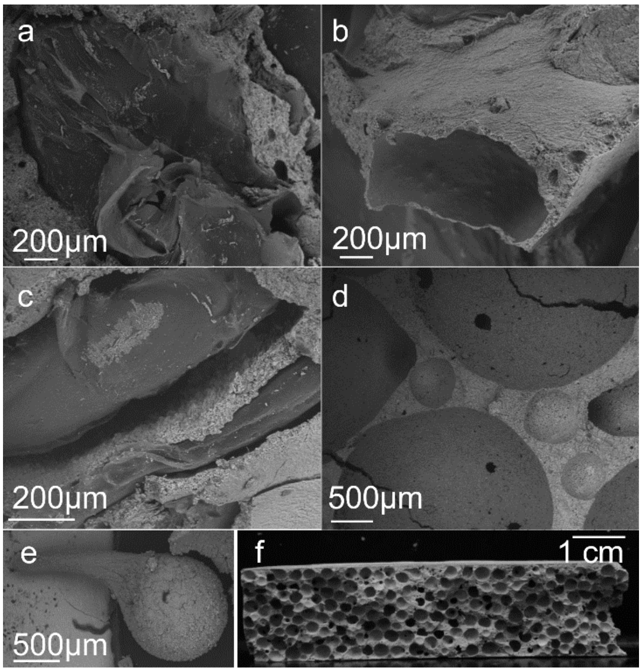

Fig. 5 SEM images of cement composite samples (a - c) where Xanthan – Konjac (2:1 ratio, total 2 wt% gelling agent) hydrogel was used, minced with 3 mm mincing plate to make the hydrogel slurry. (a) 50 vol% hydrogel, (b) 60 vol% hydrogel, (c) 70 vol% hydrogel slurry. (d) SEM image of a sample where sodium alginate (4 wt% gelling agent) hydrogel beads were used which were prepared by the syringe dripping method and gelled in 1 M $CaCl_2$ solution. The alginate beads initial content in the cement composite was 66 vol%. (e) SEM of a typical hydrogel residue particle after drying within the pore of the composite. (f) A photograph of a porous composite sample with the residues of alginate hydrogel beads after drying.

The structure of the samples produced using the sodium alginate hydrogel (produced by dropping hydrogel solution into 1M $CaCl_2$ solution to gel the drops) was found to be significantly different compared to the samples, where the blended Xanthan – Konjac hydrogels were used. This was due to the more discreet nature of the pores shown in Fig. 5 (d, f) within the samples due to the very well formed beads. We found that these composites were much more brittle than the Xanthan-Konjac hydrogel based composites, possibly due to the discreet nature of the hydrogel beads. An image of such dried alginate hydrogel particles is shown in Fig. 5(e). It was possible to image the dried beads as the beads remained within the sample, since they had no through pores to evaporate effectively and had a tendency to contract. It can also be observed that the hydrogel production technique was not refined enough to eliminate the "tail" structure observed here that occurred when the beads hit the surface of the $CaCl_2$ solution before gelling. Since the images did not show interconnected pore structure within the composite, these samples were not analysed for the sound absorption, as the sound wave would not dissipate effectively in the closed pores.

Sound absorption analysis

Samples of pure cement as well as the porous composites were tested in the sound impedance tube at least three times each and Fig. 6 shows the data obtained for the control and 50 vol% hydrogel containing samples. Under 1000 Hz the cement samples of zero hydrogel content had a poor absorption. The higher frequencies showed better absorption, especially 1400 Hz and 2000 Hz. This could be due to the fact that cement has naturally nanoporous structure, which is adequate at absorbing some of the sound energy at a particular frequency. It can be seen from these data that the porous cement samples have a markedly higher sound absorption coefficient than the control sample, particularly towards the higher sound frequency range (1000 - 2000 Hz).

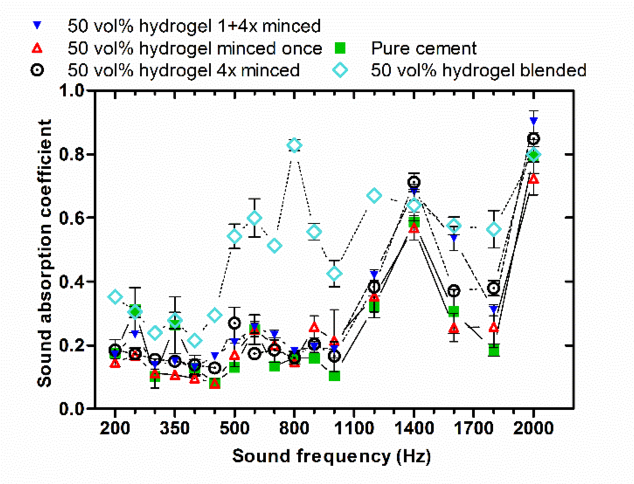

Fig. 6 Sound absorption coefficient variation at different sound frequencies for control (🟩) and 50 vol% hydrogel containing porous composites, where the hydrogel was minced once (△), four times (⦿), once and four times (1:1 ratio, ▼) and blended (◇).

A shift of the peak sound absorption was expected for the smaller beads for the 'four times minced' hydrogel slurries, but it can also be seen in Fig. 6 that the relatively small bead size change via different mincing repetitions did not influence the absorption at 50 vol% hydrogel loading within the composite. A further bead size reduction by blending did affect the sound absorption by up to 400 % at 900 Hz compared to the minced samples. This result shows that the composites produced with a smaller hydrogel bead size absorbs better these sound frequencies. As the hydrogel bead size decreased, the sound absorption increased in several frequency ranges. Higher absorption can also be seen across the around the 500 - 1200 Hz range.

For all samples, sound absorption is very high at 2000 Hz. Measurements in this region were difficult due to wave fluctuations and this could be caused by a very high level of absorption resulting in a sound wave with an amplitude which is too small to measure accurately. In future experiments, it would be beneficial to explore a wider range of sound frequencies.

We have hypothesised that the different bead size could be targeting different sound frequencies. The graphs indicate a trend of rising absorption throughout large regions, which disagreed with our expectation, demonstrating that changing bead size from 1.0 to 1.6 mm may not be suitable to target this specific range of sound frequencies. Reducing the polydispersity of the hydrogel beads and identifying this particular bead size could allow the fabrication of a very specific, monodisperse noise absorbing material, which could be useful for industrial application of the hydrogel templating technique for sound absorption. On the other hand, the reduction in hydrogel bead size did increase the overall sound absorption, making it a promising technique for fabrication of noise insulation materials.

The sound absorption coefficient was compared for various hydrogel content containing porous cement composites in Fig. 7. The porous composite samples produced with 70 vol% initial hydrogel content gave vastly improved absorption at all frequencies compared to these with 50 vol% and 60 vol% hydrogel content. Absorption in the 600 – 1200 Hz region was similar to 1800 - 2000 Hz, with $\alpha > 0.5$. Lower end frequency range absorption was also improved but not as comprehensively. Sound at 2000 Hz was almost completely absorbed, this corresponds to a material that would have excellent use as a sound proofer.

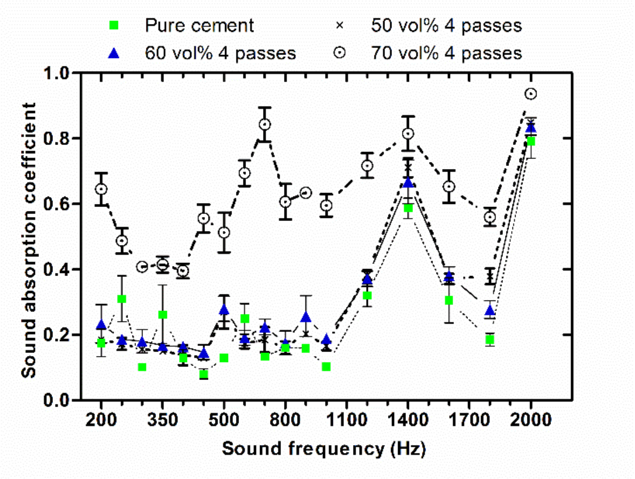

Fig. 7 Sound absorption coefficient variation across the sound frequency range for the various ratios of hydrogel used throughout the composites: 50 vol% (✕), 60 vol% (▲), 70 vol% (⦿). All hydrogels were minced four times. Control sample without the hydrogel is also shown for comparison (■). Error bars represent standard deviation for the different measurements, lines are a guide to the eye.

Compressional strength analysis

Fig. 8 shows a relatively linear trend for the samples decrease in mechanical strength and the increase in the initial hydrogel content from 50 vol% to 70 vol% within the composites. The reduction in the sample strength between 0 vol% and 50 vol% hydrogel content was more significant than between those with 50 – 70 vol% hydrogel. As expected, it is clear that the strongest material was the 100% cement sample due to a lack of induced pores. According to the literature, cement samples strength ranges from around 3 - 33MPa, depending on the type of cement and its curing stage, with rapid hardening Portland cement (also used in our study) having a 33 MPa compressive strength after 28 days [24]. Although our control sample (4 ± 1 MPa) did not match up to the upper range of these values, the porous cement samples showed considerably lower compressional strength. The high compression strength cited in the literature could be due to the addition of structure enhancing components, whereas the samples for the current study were made of pure cement slurry and added hydrogel bead slurries. Also, this study was aiming to compare like-to-like curing methods of the composites and controls, so the low compressional strength of the control sample indicates that the strength of the porous composites could be increased by 6 times using a more standardized method of preparation, setting and curing of the samples, as it is done in a specialised laboratory focused in the materials for construction purposes. Our results show that the high porosity of the samples leads to lower compressional strength. However, the acoustic absorption of the porous cement composites increases with the increased porosity which makes them promising materials for sound insulation where load bearing function is not an issue.

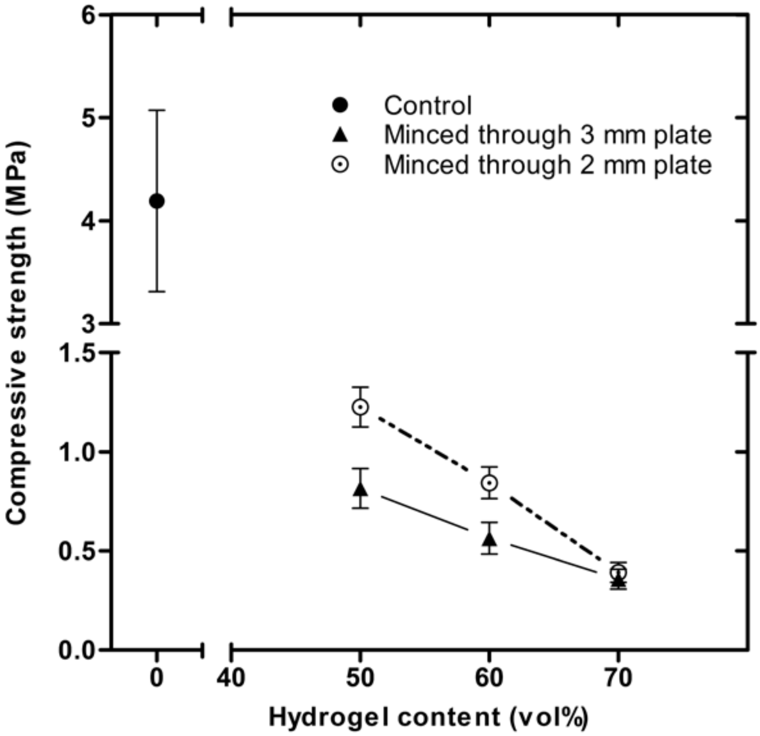

Fig. 8 Compressional strength of the data porous cement composites as a function of the initial hydrogel content before drying. Composites produced using hydrogel slurry minced through 2 mm pore size plate had a higher compressional strength compared to those from 3 mm pore size mincer plate.

Conclusions

Porous cement materials were produced by a hydrogel slurry templating technique using various volume fractions of hydrogel and different hydrogel bead sizes. The investigation of these samples through various experimental techniques resulted in the following key findings.

Hydrogel bead distribution for batches of hydrogel produced by cutting with a blender or using 2 mm and 3 mm mincer plates and passing the samples multiple times were investigated. The average size of the produced hydrogel beads ranged from 0.7 to 2.5 mm, which allowed us to control not only the porosity of the cement-hydrogel composites after drying but also their average pore size.

We showed that the hydrogel bead size has an effect on the porous cement composites sound absorption properties, with specific frequency ranges (500 - 800 Hz) being absorbed much more effectively (α between 0.50 and 0.80) using composites prepared with the blended hydrogel. These findings suggest that these porous composites have sound absorption properties similar to other porous materials described in the literature, however our materials benefit from being produced from greener technology which uses templates of hydrogels extracted from sustainable resources and have a simple fabrication method which does not involve heating of the composite.

Increasing the cement composite porosity improves its sound absorption, especially at porosity as high as 70 vol%. Pore size also has an effect on the composite sound absorption where a slight change was observed when reducing the average pore size from 1.6 mm to 1.0 mm. A much bigger improvement in the sound absorption was seen when using blended hydrogels of average bead size 0.7 mm. Modifying the pore size distribution by mixing various sized hydrogel beads batches did not seem to give any improvement in the sound absorption of the produced cement samples. We showed that increasing the hydrogel content (and therefore porosity) reduces the compressional strength of the material. The results of this study help to improve our understanding of the role of pore size and porosity on sound absorption of porous cement and can be used for manufacturing of sound insulating materials with enhanced performance.

Acknowledgements

We thank Niger Parkin for the preparation of the moulds and Iain Leishman for the assistance with compressional strength measurements. MR appreciates the EPSRC Industrial CASE award and funding from Unilever during his PhD studies.

References

[1] Passchier-Vermeer W, Passchier WF (2000) Noise exposure and public health. Environ. Health Perspect. 108: 123-131

[2] Mead MN (2007) Noise pollution: the sound behind heart effects. Environ. Health Perspect. 115: A536-A537

[3] Godlee F (1992) Noise: breaking the silence. Brit Med J 304: 110-113

[4] Ma G, Yang M, Xiao S, Yang Z, Sheng P (2014) Acoustic metasurface with hybrid resonances. Nat. Mater. 13: 873-878

[5] Yilmaz ND, Banks-Lee P, Powell NB, Michielsen S (2011) Effects of Porosity, Fiber Size, and Layering Sequence on Sound Absorption Performance of Needle-Punched Nonwovens. J. Appl. Polym. Sci. 121: 3056-3069
[6] Sagartzazu X, Hervella-Nieto L (2011) Impedance prediction for several porous layers on a moving plate: application to a plate coupled to an air cavity. Journal of Computational Acoustics 19: 379-394
[7] Crocker MJ (2007) Handbook of Noise and Vibration Control. John Wiley & Sons, Hoboken, New Jersey
[8] Beranek LL, Vér IL (1992) Noise and vibration control engineering: principles and applications. John Wiley & Sons, New York, New York
[9] Cox TJ, D'Antonio P (2004) Acoustic Absorbers and Diffusers: Theory, Design and Application. Taylor & Francis, London, UK
[10] Fahy FJ (2000) Foundations of Engineering Acoustics. Elsevier Science, London, UK
[11] Arenas JP, Crocker MJ (2010) Recent Trends in Porous Sound-Absorbing Materials. Sound Vib 44: 12-17
[12] Maa D-Y (1998) Potential of microperforated panel absorber. The Journal of the Acoustical Society of America 104: 2861-2866
[13] Olny X, Boutin C (2003) Acoustic wave propagation in double porosity media. The Journal of the Acoustical Society of America 114: 73-89
[14] Laukaitis A, Fiks B (2006) Acoustical properties of aerated autoclaved concrete. Appl. Acoust. 67: 284-296
[15] Atalla N, Panneton R, Sgard FC, Olny X (2001) Acoustic absorption of macro-perforated porous materials. J. Sound Vib. 243: 659-678
[16] Glé P, Gourdon E, Arnaud L (2011) Acoustical properties of materials made of vegetable particles with several scales of porosity. Appl. Acoust. 72: 249-259
[17] Karabulut S, Caliskan M (2013) Development of an ecological, smooth, unperforated sound absorptive material. Proceedings of Meetings on Acoustics 19: 1-7
[18] Cuiyun D, Guang C, Xinbang X, Peisheng L (2012) Sound absorption characteristics of a high-temperature sintering porous ceramic material. Appl. Acoust. 73: 865-871
[19] Sgard FC, Olny X, Atalla N, Castel F (2005) On the use of perforations to improve the sound absorption of porous materials. Appl. Acoust. 66: 625-651
[20] Rutkevičius M, Munusami SK, Watson Z, et al. (2012) Fabrication of novel lightweight composites by a hydrogel templating technique. Mater. Res. Bull. 47: 980-986
[21] Rutkevičius M, Mehl GH, Paunov VN, et al. (2013) Sound absorption properties of porous composites fabricated by a hydrogel templating technique. J. Mater. Res. 28: 2409-2414
[22] Organisation IS (1996) ISO 10534-1:1996: Acoustics - Determination of sound absorption coefficient and impedance in impedance tubes. Part 1: Method using standing wave ratio. Geenva, Switzerland
[23] Kistler SS (1931) Coherent Expanded Aerogels and Jellies. Nature 127: 741-741
[24] Charlett AJ, Craig MT (2006) Fundamental Building Technology. Taylor & Francis, Oxon, UK